A CONSTITUTIVE MODEL FOR REPRESENTING COUPLED CREEP, FRACTURE, AND HEALING IN ROCK SALT*

Kwai S. Chan
Southwest Research Institute, San Antonio, TX 78238
Darrell E. Munson
Sandia National Laboratories, Albuquerque, NM 87185**
Arlo F. Fossum
Sandia National Laboratories, Albuquerque, NM 87185
Sol R. Bodner†
Southwest Research Institute, San Antonio, TX 78238

ABSTRACT

The development of a constitutive model for representing inelastic flow due to coupled creep, damage, and healing in rock salt is presented in this paper. This constitutive model, referred to as Multimechanism Deformation Coupled Fracture (MDCF) model, has been formulated by considering individual mechanisms that include dislocation creep, shear damage, tensile damage, and damage healing. Applications of the model to representing the inelastic flow and fracture behavior of WIPP salt subjected to creep, quasi-static loading, and damage healing conditions are illustrated with comparisons of model calculations against experimental creep curves, stress-strain curves, strain recovery curves, time-to-rupture data, and fracture mechanism maps.

INTRODUCTION

This effort was motivated by the projected use of excavated rooms in natural rock salt formations as repositories for nuclear waste. A complete isolation of the waste in salt from the environment is enhanced by (1) encapsulation of the waste material by room closure due to salt creep, and (2) an effective sealing system in the shafts that connect to the underground rooms. Creep of salt, however, can induce the formation of microcracks under low confinement conditions. Pre-existing microcracks might also be introduced in salt during excavation. The presence of damage in the form of microcracks in salt can alter the structural stability and the permeability of salt, affecting the integrity of a repository. Thus, the development and healing of damage in salt are important factors affecting waste isolation. An accurate prediction of the encapsulation process, the effectiveness of the seal systems, and the structural

* Work supported by the U. S. Department of Energy (DOE) under Contract No. DE-AC94-AL85000
** A DOE facility
† Permanent address: Technion, Dept. Mech. Eng., Haifa, Israel

performance of the repository requires that the creep and damage characteristics of salt be characterized and modeled.

Constitutive equations for creep of salt are fairly well established and compared favorably with field measurements. Now, significant steps have been taken in the simulation of fracture and healing. Both uncoupled (Cristescu and Hunsche [1992]; Cristescu [1993]) and coupled (unified) (Munson and Dawson [1984]; Munson et al. [1989]; Aubertin et al. [1991, 1993]) plasticity/creep models have been developed. Time-dependent damage has been incorporated into some formulations (Chan et al. [1992, 1994]; Aubertin et al. [1993]) through the use of the isotropic damage variable in the context of Kachanov (1958). Damage was considered both as a modifier to the load-bearing area and a direct contributor to the inelastic strain rate. This approach has allowed damage-induced inelastic flow to commence in the transient creep regime and develop into tertiary creep as damage accumulates without a true steady-state creep regime.

The constitutive model developed by the authors was intended for treating coupled creep, fracture, and healing in rock salt. This model was first developed as a set of constitutive equations, referred to as the Multimechanism Deformation (M-D) model, for treating salt creep due to dislocation flow mechanisms (Munson and Dawson [1984]; Munson et al. [1989]). Hardening and recovery of hardening were treated using an isotropic hardening variable, leading to representation of both transient and steady-state creep behaviors. Tertiary creep was represented by extending the M-D model to include the evolution of damage during deformation. The extended model, referred to as the Multimechanism Deformation Coupled Fracture (MDCF) model, was formulated by incorporating continuum, isotropic damage as a fully coupled variable that enhances the stress influence by reduction of the effective area and contributes directly to the inelastic strain rate (Chan et al. [1992, 1994, 1996a]). The total elastic strain rate equation thereby becomes pressure dependent because the subsidiary equations include the effect of pressure to suppress damage development. Damage healing by a hydrostatic pressure was formulated and incorporated in the latest model development (Chan et al. [1995a]).

In this paper, the formulation of the MDCF model is summarized. Applications of the proposed model to representing the inelastic flow and fracture behaviors of WIPP salt subjected to various loading conditions are presented. Specifically, the constitutive model was utilized to compute the stress-strain responses under triaxial compression creep, constant rate compression, and damage healing by hydrostatic compression. The capabilities of the model for predicting creep, fracture, and healing responses of WIPP salt are illustrated with comparisons of model calculations against experimental creep curves, stress-strain curves, strain recovery curves, time-to-failure data, and fracture mechanism maps.

SUMMARY OF THE MDCF MODEL

The constitutive equations have been formulated on the basis that the total strain rate, $\dot{\epsilon}_{ij}^{T}$, is composed of an elastic term, $\dot{\epsilon}_{ij}^{E}$, and an inelastic term, $\dot{\epsilon}_{ij}^{I}$, according to

$$\dot{\epsilon}_{ij}^{T} = \dot{\epsilon}_{ij}^{E} + \dot{\epsilon}_{ij}^{I} \tag{1}$$

in which the elastic strain rate is given by the generalized Hooke's law and the inelastic term is intended to treat all aspects of inelasticity. The generalized form of the inelastic strain rate is given by (Fossum et al. [1988])

$$\dot{\epsilon}_{ij}^{I} = \frac{\partial \sigma_{eq}^{\alpha}}{\partial \sigma_{ij}} \dot{\epsilon}_{eq}^{\alpha} \tag{2}$$

where σ_{eq}^{α} and $\dot{\epsilon}_{eq}^{\alpha}$ are the power-conjugate equivalent stress and strain rate measures, respectively, for deformation mechanism α, with α = 1, 2, 3, ..., n, in a solid that exhibits n deformation mechanisms. This generalized flow law has been derived based on a thermodynamic formulation in which the power-conjugate equivalent stress measure plays the role of a flow potential and the derivative with stress, σ_{ij}, defines the flow direction.

Inelastic flow in rock salt occurs by dislocation, microfracture, and damage healing mechanisms. The process driving forces for individual flow mechanisms are represented by appropriate power-conjugate equivalent stress measures, from which appropriate flow laws are derived and summed according to Eq. (2). Thus, the overall flow law is (Chan et al. [1992, 1994, 1995a])

$$\dot{\epsilon}_{ij}^{I} = \frac{\partial \sigma_{eq}^{c}}{\partial \sigma_{ij}} \dot{\epsilon}_{eq}^{c} + \frac{\partial \sigma_{eq}^{\omega_s}}{\partial \sigma_{ij}} \dot{\epsilon}_{eq}^{\omega_s} + \frac{\partial \sigma_{eq}^{\omega_t}}{\partial \sigma_{ij}} \dot{\epsilon}_{eq}^{\omega_t} + \frac{\partial \sigma_{eq}^{h}}{\partial \sigma_{ij}} \dot{\epsilon}_{eq}^{h} \tag{3}$$

for coupled creep (c), shear damage (ω_s), tensile damage (ω_t), and damage healing (h). The superscripts to the equivalent strain rate, $\dot{\epsilon}_{eq}$, and the power-conjugate stress measure, σ_{eq}, indicate quantities corresponding to individual mechanisms. A summary of the conjugate equivalent stress and strain rate measures for individual deformation mechanisms is presented next.

(1) Conjugate Equivalent Stress Measures

Inelastic flow due to dislocation creep is isochoric and pressure-independent. These features lead to a conjugate equivalent stress measure for dislocation creep, σ_{eq}^{c}, which is formulated based on the stress difference as given by (Munson and Dawson [1984]; Munson et al. [1989])

$$\sigma_{eq}^{c} = |\sigma_1 - \sigma_3| \tag{4}$$

where σ_1 and σ_3 are the maximum and minimum principal stresses, with compression being positive. The Tresca equivalent stress measure is preferred over that of von Mises because experimental measurements of the flow surface and inelastic strain rate vector are in better agreement with the former formulation (Munson et al. [1989]).

Damage development in compression is considered to arise from sliding of microcracks by shear and the opening of wing-tip cleavage cracks that develop on some of the shear cracks. The resulting inelastic flow includes deviatoric and dilatational components with a pressure dependence. These characteristics have been accounted for in a nonassociated flow formulation by using two conjugate equivalent stress measures, one for the flow law and another for the kinetic equation. These stress measures are (Chan et al. [1992, 1994, 1996a])

$$\left[\sigma_{eq}^{\omega_s}\right]_f = |\sigma_1 - \sigma_3| - x_2 x_8 [I_1 - \sigma_1]/3 \tag{5}$$

for the flow law and

$$\left[\sigma_{eq}^{\omega_s}\right]_k = |\sigma_1 - \sigma_3| - x_2 x_7 sgn(I_1 - \sigma_1)\left[\frac{I_1 - \sigma_1}{3x_7 sgn(I_1 - \sigma_1)}\right]^{x_6} \tag{6}$$

for the kinetic equation; where I_1 is the first invariant of Cauchy stress; the x_i's are material constants; sgn( ) is the signum function. The first terms on the RHS of Eqs. (5) and (6) represent shear-induced damage, which manifests as slip-induced shear microcracks. Some of these microcracks develop wing tips that generate irreversible inelastic strains that add to those originating from dislocation flow mechanisms. Opening of these wing cracks, which are aligned parallel to the maximum principal stress (σ_1), occurs in directions normal to the σ_1 direction and is resisted by compressive stresses of σ_2 and σ_3. The second terms in the RHS of Eqs. (5) and (6), which are in the form of f($I_1 - \sigma_1$), model the effects of stress state on aiding or suppressing the opening of wing cracks.

Tensile creep damage in salt occurs in the form of cleavage microcracks aligned normal to the tensile stress. The kinetics of tensile damage in salt is substantially faster than shear damage and is therefore treated as a separate term. The conjugate equivalent stress measure for tensile damage-induced flow is (Chan et al. [1996a])

$$\sigma_{eq}^{\omega_t} = -x_1 \sigma_3 H(-\sigma_3) \tag{7}$$

where H( ) denotes the Heaviside step function. This stress measure is intended to represent the opening of microcracks by a tensile stress, σ_3.

Reduction of damage in rock salt can occur by the closure of open microcracks and the sintering of microcracks. Both of these processes can be considered to be driven by an identical thermodynamic driving force represented by a pertinent

power-conjugate equivalent stress measure. If the healing process is isotropic, the appropriate power-conjugate equivalent stress measure is the first invariant, I_1, of the Cauchy stress. On the other hand, damage healing might be nonisotropic or exhibit induced anisotropy. For this situation, a second stress term in addition to I_1 is required. For describing stress-induced healing anisotropy, the conjugate equivalent stress measure for damage healing may be taken as (Chan et al. [1995a])

$$\sigma^{h}_{eq} = \frac{1}{3}(I_1 - x_{10}\sigma_1) \tag{8}$$

where x_{10} is a material constant. One of the characteristics of this conjugate equivalent stress measure is that when used in conjunction with Eq. (3), the healing term is the only nonzero term under hydrostatic compression. But, in addition, healing may also occur under nonhydrostatic compression.

(2) Equivalent Strain Rate Measures

The kinetic equation representing the creep rate, $\dot{\epsilon}^{c}_{eq}$, due to dislocation flow mechanisms was formulated by Munson and Dawson (1984) and is given by

$$\dot{\epsilon}^{c}_{eq} = F \sum_{i=1}^{3} \dot{\epsilon}_{s_i} \tag{9}$$

where F is the transient function representing transient creep behavior, $\dot{\epsilon}_{s_i}$ is the steady state strain rate for the i^{th} independent dislocation flow mechanism. The mechanisms include dislocation climb (i = 1), dislocation glide (i =3), and one that has not been identified mechanistically but which is fully characterized experimentally (i = 2). The steady state strain rates are (Munson and Dawson [1984])

$$\dot{\epsilon}_{s_i} = A_i e^{-Q_i/RT} \left[\frac{\sigma^{c}_{eq}}{\mu(1 - \omega)} \right]^{n_i} \tag{10}$$

for i = 1, and 2, and

$$\dot{\epsilon}_{s_3} = |H| \left(\sum_{i=1}^{2} B_i e^{-Q_i/RT} \right) \sinh\left[\frac{q}{\mu} \left(\frac{\sigma^{c}_{eq}}{1 - \omega} - \sigma_o \right) \right] \tag{11}$$

for i = 3; where the A_i's and B_i's are constants; Q_i's are activation energies; T is absolute temperature; R is the universal gas constant; μ is shear modulus; n_i's are the stress exponents; q is the stress constant; H is the Heaviside function with $[\sigma^{c}_{eq}/(1-\omega) - \sigma_o]$ as the argument; and σ_o is the stress limit of the dislocation glide mechanism.

The kinetic equation of damage-induced inelastic flow was developed on the basis that wing cracks developed at the tips of sliding shear cracks or slipbands. As a result, the kinetic equation for shear-induced damage followed closely to that for

dislocation glide. The same form of expression was also used for the kinetic equation for tensile damage-induced flow and is given by (Chan et al. [1994, 1996a])

$$\dot{\epsilon}_{eq}^{\omega_i} = F^{\omega_i} \dot{\epsilon}_s^{\omega_i} \tag{12}$$

where i = s or t for shear or tensile damage, respectively; F^{ω_i} is the transient function for the i^{th} mode of damage. The kinetic equations for damage-induced flow, $\dot{\epsilon}_s^{\omega_i}$, during steady-state creep are expressed by

$$\dot{\epsilon}_s^{\omega_i} = c_o \left(\sum_{i=1}^{2} B_i e^{-Q_i/RT} \right) \omega_o e^{c_3 \omega} \left[\sinh \left(\frac{c_2 \sigma_{eq}^{\omega_i} H(\sigma_{eq}^{\omega_i})}{(1-\omega)\mu} \right) \right]^{n_3} \tag{13}$$

where c_i's and n_3 are material constants and ω_o is the initial value of the damage variable, ω. The kinetic equation in Eq. (12) allows $\dot{\epsilon}_{eq}^{\omega_i}$ to exhibit a transient behavior by virtue of the transient function, F^{ω_i}, which is directly related to the transient function, F, for creep. The expressions for the transient functions can be found in earlier publications (Chan et al. [1994, 1996a]).

Experimental evidence indicated that two healing mechanisms might be present in WIPP salt. Each of the two healing mechanisms may be described by a first-order kinetic equation. The first mechanism, which is closure of microcracks, has a smaller time constant, τ_1, than the time constant, τ_2, for the second mechanism, which is healing of microcracks. The kinetic equation for damage healing in WIPP salt is taken to be (Chan et al. [1996b])

$$\dot{\epsilon}_{eq}^{h} = \frac{\epsilon_{kk} (\sigma_{eq}^{h} - \sigma_{th}) H\left(\sigma_{eq}^{h} - \sigma_{th}\right)}{\tau \mu} \tag{14}$$

where ϵ_{kk} is the volumetric strain, σ_{th} is the threshold stress for healing, and τ is the characteristic time for damage healing. According to Eq. (14), damage healing takes place only when $\sigma_{eq}^{h} > \sigma_{th}$ and it tends to reduce ϵ_{kk} to zero. The threshold stress, σ_{th}, is introduced so that damage healing and damage development do not occur concurrently. To account for two characteristic times, τ is taken to be a function of the volumetric strain such that the characteristic time, τ, approaches τ_1 when the volumetric strain becomes large but approaches τ_2 when the reverse is true.

(3) Damage Evolution Equations

An internal damage variable in the context of Kachanov's isotropic damage parameter, ω, was used as a measure of the current state of damage in the deformed solid. Damage development in the MDCF model is then described in terms of an evolution equation that contains both damage growth and healing terms, as given by (Chan et al. [1995a])

$$\dot{\omega} = g(\omega, T, \sigma_{eq}^{\omega_i}, \chi_i) - h(\omega, T, \sigma_{eq}^{h}) \tag{15}$$

where $g(\omega, T, \sigma_{eq}^{\omega_i}, \chi_i)$ describes the growth of damage, and $h(\omega, T, \sigma_{eq}^{h})$ describes the healing of damage. The damage growth function, g, is given by (Chan et al, [1994, 1996a])

$$g = \frac{x_4}{t_o}\omega\left[\ln\left(\frac{1}{\omega}\right)\right]^{\frac{x_4+1}{x_4}}\left\{\left[\frac{\sigma_{eq}^{\omega_s} H(\sigma_{eq}^{\omega_s})}{\chi_s}\right]^{x_{3s}} + \left[\frac{\sigma_{eq}^{\omega_t} H(\sigma_{eq}^{\omega_t})}{\chi_t}\right]^{x_{3t}}\right\} \tag{16}$$

where x_{3i}, x_4, χ_i (with i = s or t for shear or tensile damage, respectively) are material constants, and t_o is a reference time. Motivated by the experimental observations (Brodsky and Munson [1994], Chan et al. [1996b]) the healing function is taken to be a first-order kinetic equation given by

$$h = \frac{\omega\,(\sigma_{eq}^{h} - \sigma_{th})\,H\,(\sigma_{eq}^{h} - \sigma_{th})}{\tau\,\mu} \tag{17}$$

which has the same form as the kinetic equation for damage healing, Eq. (14). The overall evolution equation for damage with healing is obtained by combining Eq. (15) with Eqs. (16) and (17).

APPLICATION OF THE MDCF MODEL

The utilities of the MDCF model are demonstrated here for creep, quasi-static compression, and healing conditions, followed by applications of the model to calculating fracture mechanism maps for WIPP salt. The use of the model in conjunction with a finite-element code for predicting the failure of excavated rooms at the WIPP is presented earlier (Chan et al. [1995b]). The material constants in the MDCF model were determined by fitting model calculations to experimental creep curves of WIPP salt. The material constants for WIPP clean and argillaceous salt are presented elsewhere (Chan et al. [1996a]). This same set of material constants was used for the calculations shown here.

Coupling of creep and damage in the MDCF model allowed calculation of the entire creep curves, including tertiary creep, of WIPP clean and argillaceous salt. Calculated creep curves for WIPP clean salt tested at a stress difference of 25 MPa under a confining pressure of 1 or 15 MPa are compared against the experimental data in Figure 1. The agreement between model calculation and experimental data is considered good because it is within the variability factor of two usually observed in the experimental creep curves. Both the calculated and measured creep responses were dilatational at 1 MPa confining pressure, but were isochoric at 15 MPa confining pressure. This pressure dependence was the result of damage development being totally suppressed at the higher confining pressure.

Using the MDCF model, the creep rupture responses of WIPP salt in triaxial compression were calculated and compared with experimental data in Figure 2.

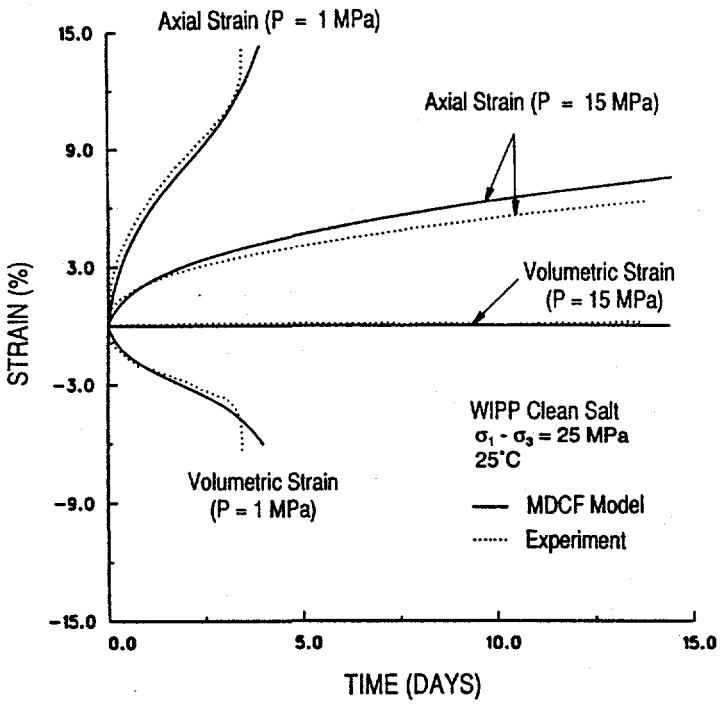

Figure 1. Experimental creep curves of WIPP salt tested at $\sigma_1-\sigma_3 = 25$ MPa under a confining pressure, P, of 1 or 15 MPa with comparison to model calculations. (From Chan et al. [1994].)

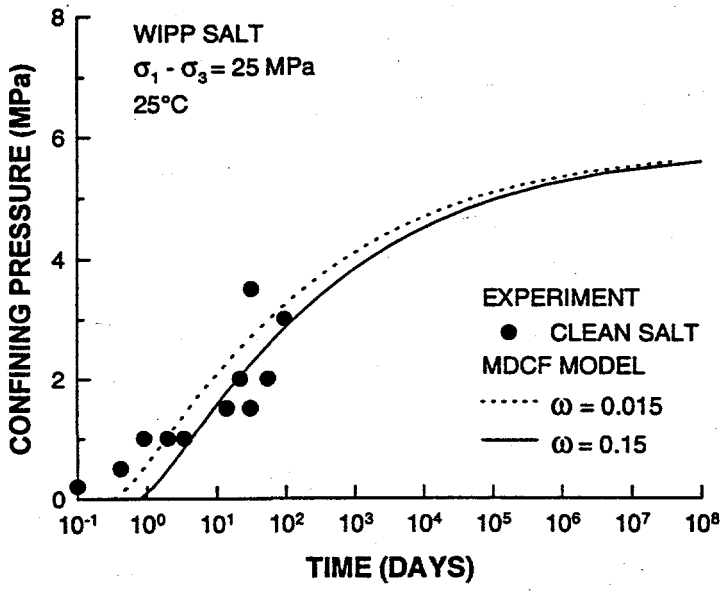

Figure 2. Comparison of calculated and measured time-to-rupture results of WIPP salt as a function of confining pressure. The onset of tertiary creep was taken to commence at $\omega = 0.015$ and creep rupture was taken to occur at $\omega = 0.15$ in the model calculations. (From Chan et al. [1996a].)

Extrapolation to very long time, as shown in Figure 2, is typical of the requirement for this predictive technique. Triaxial compression creep tests were conducted on cylindrical specimens at a stress difference of 25 MPa under various confining pressures. The calculated time-to-rupture values were based on critical damage values of 0.015 and 0.15. Figure 2 suggests that a critical value of $\omega = 0.015$ may be used as a criterion for representing the onset of tertiary creep. Furthermore, a critical value of $\omega = 0.15$ may be used as the criterion for creep rupture in WIPP salt.

The MDCF model has been formulated based on the unified constitutive approach in which both plasticity and creep are treated using the same set of flow laws, kinetic equations, and evolution equations of the internal variables. Consequently, plastic flow can be modeled without the use of yield and loading/unloading criteria. This is demonstrated by a calculation of the stress-strain response of WIPP salt subjected to a low confining pressure (0.5 MPa) at a constant strain rate of 1×10^{-6} sec^{-1} at 25°C. Comparison of the model calculation and experimental stress-strain curves is presented in Figure 3, which shows stresses as functions of the axial and lateral strains. Volumetric strains were observed during compression of WIPP salt. The calculated volumetric strain was also in agreement with the observed value.

The MDCF model was used to calculate the stress-strain and damage responses during damage healing of WIPP salt. In both the healing experiment (Brodsky and Munson, [1994]) and model calculation, WIPP salt was prestrained to 1.5% axial strain under a strain rate of 1×10^{-6} sec^{-1} and 0.5 MPa confining pressure. After reaching 1.5% total strain, the axial stress was reduced to 0.5 MPa and subsequently the hydrostatic pressure was increased to 15 MPa. The axial, lateral, and volumetric strains recovered during damage healing of WIPP salt at 20°, 46°, and 70°C were calculated. Figure 4 shows comparison of the calculated and measured axial, lateral, and volumetric strains recovered as a function of time of healing at 46°C. The results show that the healing responses are reasonably well described by the model for both short and long durations. The amount of volumetric strain recovered by damage healing was quite rapid at short times of healing. This rapid healing behavior is thought to arise from the closure of open microcracks. At longer times of healing, the rate of healing is slower; the amount of volumetric strain recovered increases with temperature and with time of healing, which is consistent with sintering of microcracks by a diffusion controlled process.

Both the experiment and model calculations showed anisotropic healing as the axial, lateral, and volumetric strains were substantially different from those expected on the basis of isotropic healing. In particular, isotropic healing would lead to a compressive strain in the axial direction. Experimental measurements, however, revealed a tensile axial strain during healing, thus indicating the development of anisotropy during damage healing. The recovery of strains was directly related to the

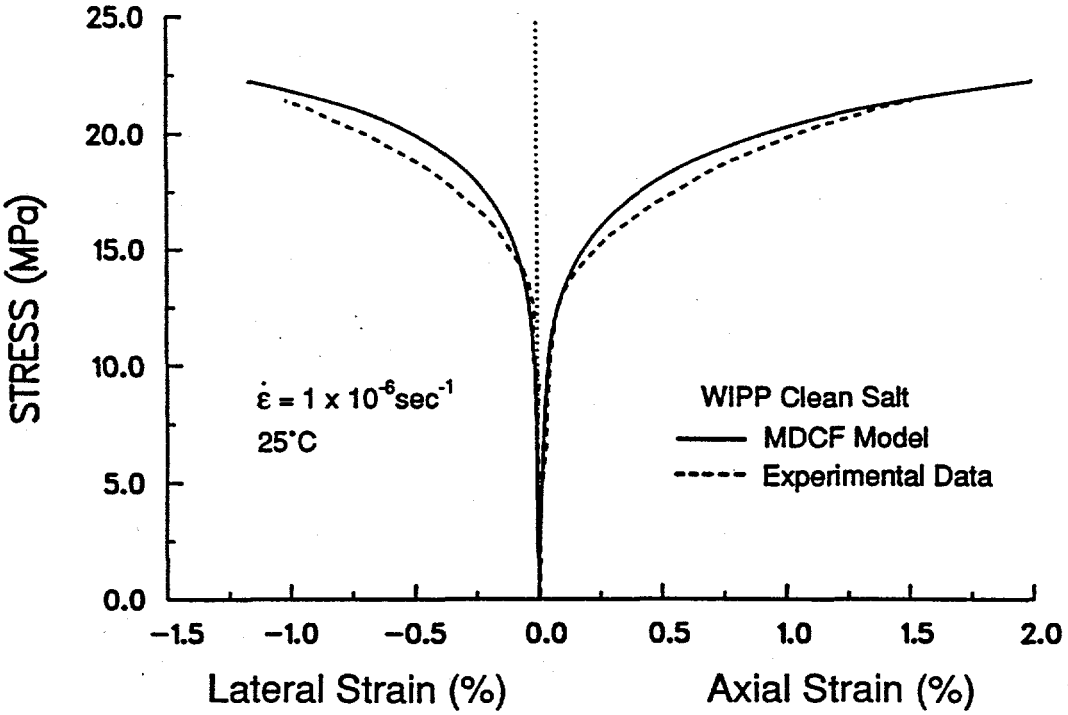

Figure 3. Calculated and experimental stress-strain curves for WIPP salt tested under a constant strain rate of 1×10^{-6} sec^{-1} at 25°C. (From Chan et al. [1996b].)

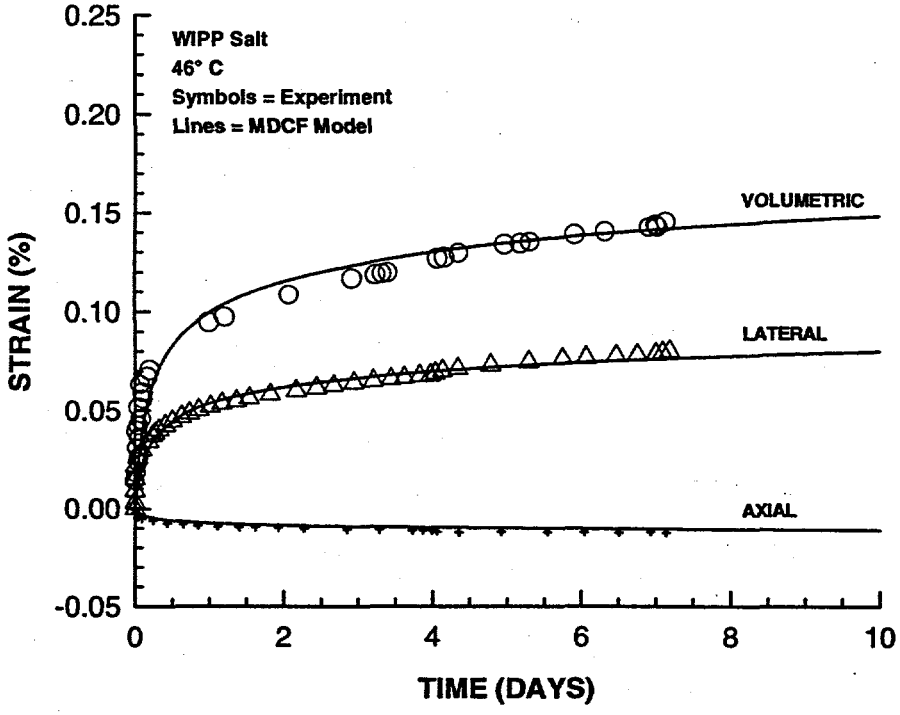

Figure 4. Measured volumetric, lateral, and axial strains recovered during damage healing of WIPP salt under a hydrostatic pressure of 15 MPa at 46°C with model calculations. (From Chan et al. [1996b].)

reduction of damage during healing, which was verified by in-situ measurements of ultrasonic wave velocity (Brodsky and Munson [1994]; Chan et al. [1995a]).

The fracture mechanisms in WIPP salt at ambient temperature are cleavage and creep fracture. The failure boundaries of both cleavage and creep fracture were calculated using a wing-crack model and the MDCF model (Chan et al. [1996c]). The results are presented in the form of a fracture mechanism map in Figure 5, which shows the failure boundaries in the stress space of $-\sigma_1$ and $-\sigma_3$. The dashed/dotted line represents the stress loci within which isochoric creep without damage occurs. The solid line represents the cleavage fracture loci at which unstable cleavage fracture occurs. The region between the dashed/dotted line and the solid line depicts stress states where dilatational creep with damage and creep fracture would occur after an unspecified time of creep. The calculated fracture mechanism map is in good agreement with experimental data of rock salt from various sources (Brodsky [1995]; Hunsche [1993]; Skrotzki and Haasen [1984]; Stokes [1966]; Van Sambeek et al. [1993]; Fossum et al. [1993]; Wawersik and Hannum [1979]), as shown in Figure 5.

A fracture mechanism map was also calculated for the stress space of stress difference and confining pressure, σ_3 ($=\sigma_2=P$) and the result is presented in Figure 6 (Chan et al. [1996c]). The cleavage fracture boundaries were calculated on the basis of a wing crack model and the Griffith fracture criterion. The failure boundaries of the creep damage mechanisms were described in terms of isochronous failure curves, which are stress contours of constant creep rupture time. The isochronous failure curve with a failure time of infinity was used to define the boundary between regions where creep occurs with and without damage. Isochronous curves of a time-to-rupture of one hour were used to depict failure regimes where creep crack growth is expected to dominate due to the short failure time. On this basis, the fracture mechanism map in Figure 6 is divided into seven failure regimes; (1) Region A, where isochoric creep occurs without rupture; (2) Region C, where dilatational flow occurs with microcrack damage; (3) Region D, where fracture occurs by wing-crack extension; (4) Region E, where creep failure occurs by a mixture of tensile and shear damage; (5) Region F, where tensile creep crack growth dominates; (6) Region G, where cleavage fracture by wing crack dominates; and (7) Region H, where cleavage fracture by the Griffith crack dominates. Comparison of the calculated fracture mechanism map with experimental data of WIPP salt (Van Sambeek et al. [1993]; Senseny [1986]; Fossum et al. [1993]; Wawersik and Hannum; and Brodsky [1995]) and ASSE salt (Hunsche [1993]) in Figure 6 shows that the calculated cleavage and creep fracture boundaries agree with both sets of experimental data.

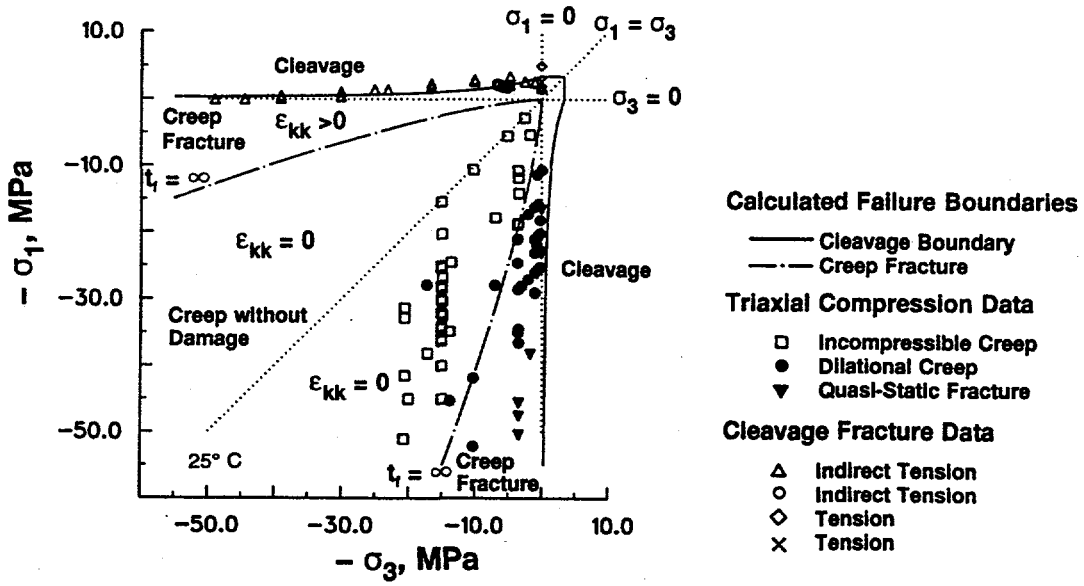

Figure 5. Comparison of calculated fracture mechanism map against experimental data of rock salt. The cleavage fracture data are from Brodsky [1995], Hunsche [1993], Skrotzki and Haasen [1984], and Stokes [1966]. The triaxial compression data are from Van Sambeek et al. [1993], Senseny [1986], Fossum et al. [1993], Wawersik and Hannum [1979]. (From Chan et al. [1996c].)

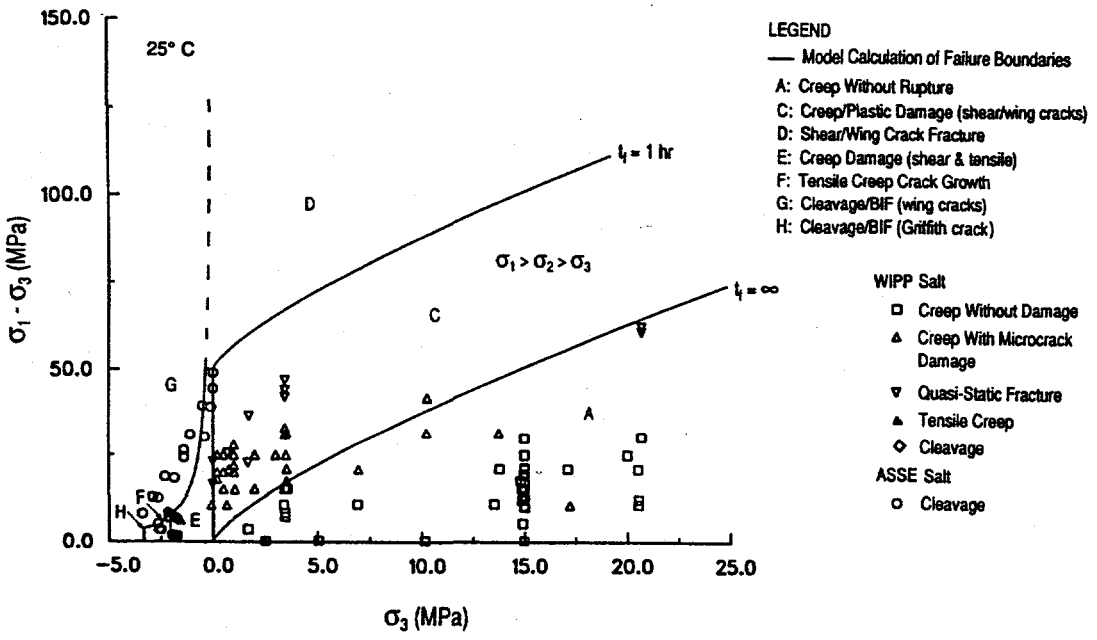

Figure 6. Computed fracture mechanism map compared against experimental data of WIPP salt (Brodsky [1995]; Van Sambeek et al. [1993]; Senseny [1986]; Fossum et al. [1993]; Wawersik and Hannum [1979]) and ASSE salt (Hunsche [1993]). (From Chan et al. [1996c].)

SUMMARY

The development of the Multimechanism Deformation Coupled Fracture (MDCF) model for treating coupled creep, damage, and healing in rock salt is summarized. Formulations of flow laws, kinetic equations, and evolution equations of internal variables are presented for individual mechanisms, which include dislocation creep, shear damage, tensile damage, and damage healing. Applications of the model to describing the inelastic flow and fracture behaviors of WIPP salt subjected to creep, constant strain rate compression, and damage healing are demonstrated. The capabilities of the model are illustrated by comparing model calculations against experimental creep curves, stress-strain curves, strain recovery curves, time-to-rupture data, and fracture mechanism maps.

REFERENCES

Aubertin, M., Gill, D. E., and Ladanyi, B., [1991], Mech. of Mat., Vol. 11, 63-82.

Aubertin, M., Sgaoula, J., and Gill, D. E., [1993], in 7th Symp. on Salt, Vol. 1, H. Kakihana, et al. (eds), Elsevier Science Publications, New York, NY, 117-125.

Brodsky, N. S., [1995], RE/SPEC Inc., Rapid City, South Dakota 57709, "Personal Communication."

Brodsky, N. S. and Munson, D. E., [1994], in Proc. First N. Amer. Rock Mech. Symp., P. P. Nelson and S. E. Laubach (eds), Balkema, Brookfield, VT, 731-738.

Chan, K. S., Bodner, S. R., Fossum, A. F. and Munson, D. E., [1992], Mech. Mat. Vol 14, 1-14.

Chan, K. S., Brodsky, N. S., Fossum, A. F., Bodner, S. R., and Munson, D. E., [1994], Int. J. of Plasticity, Vol. 10, 623-642.

Chan, K. S., Bodner, S. R., Fossum, A. F., and Munson, D. E., [1995a], in Proceedings of the 35th U. S. Symposium on Rock Mechanics, J. J. K. Daemen and R. A. Schultz (eds), Balkema, Brookfield, VT, 485-490.

Chan, K. S., DeVries, K. L., Bodner, S. R., Fossum, A. F., and Munson, D. E., [1995b] in Computational Mechanics '95, S. N. Atluri, G. Yagawa and T. A. Cruse (eds), Springer, Berlin, 1140-1145.

Chan, K. S., Bodner, S. R., Fossum, A. F., and Munson, D. E., [1996a], Int. J. Damage Mechanics, (in press).

Chan, K. S., Munson, D. E., Bodner, S. R., [1996b], submitted for publication.

Chan, K. S., Munson, D. E., Fossum, A. F., and Bodner, S. R., [1996c], Acta Metall. et Mater., (in press).

Cristescu, N., [1993], Int. J. Rock Mech. Mining Sciences & Geomech. Abstr. Vol. 30, 125-140.

Fossum, A. F., Callahan, G. D., Van Sambeek, L. L., and Senseny, P., [1988], in Key Questions in Rock Mechanics, P. A. Cundall, R. L. Sterling, and A. M. Starfield (eds), Balkema, Brookfield, VT, 35-41.

Fossum, A. F., Brodsky, N. S., Chan, K. S., and Munson, D. E., [1993], Int. J. of Rock Mech. Mining Sciences & Geomech. Abstr. Vol. 30, 1341-1344.

Hunsche, U. E., [1993], in 7th Symp. on Salt, Vol. 1, H. Kakihana, et al. (eds), Elsevier Science Publication, New York, NY, 59-65.

Kachanov, L. M., [1958], Izv. Akad. Nauk SSSR. Tekh, Vol. 8, Nauk: Otdgel., 26-31 (in Russian).

Munson, D. E., and Dawson, P. R., [1984], Proc. First Conf. on the Mechanical Behavior of Salt, Trans. Tech. Publications, Clausthal, Germany, 717-737.

Munson, D. E., Fossum, A. F., and Senseny, P. E., [1989], Advances in Resolution of Discrepancies Between Predicted and Measured In-Situ WIPP Room Closures, Report SAND88-2948, Sandia National Laboratories, Albuquerque, New Mexico.

Senseny, P.E., [1986], Triaxial Compression Creep Tests on Salt From the Waste Isolation Pilot Plant, Report SAND85-7261, Sandia National Laboratories, Albuquerque, New Mexico.

Skrotzki, W., and Haasen, P., [1984], in Deformation of Ceramic Materials II, R. Tressler and R. C. Brandt (eds), Mat. Sci. Res., Vol. 18, Plenum Press, New York, NY, 429-444.

Stokes, R. J., [1966], Proc. British Ceram. Soc., Vol. 6, 189-207.

Van Sambeek, L. L., Fossum, A. F., Callahan, G., and Ratigan J., [1993] in 7th. Symp. on Salt, Vol. 1, H. Kakihana, et al. (eds), Elsevier Science Publications, New York, NY, 127-134.

Wawersik, W. R., and Hannum, D. W., [1979] Interim Summary of Sandia Creep Experiments on Rock Salt From the WIPP Study Area, Southwest New Mexico, Report SAND79-0115, Sandia National Laboratories, Albuquerque, New Mexico.

DISCLAIMER